SLA Printed K-Band Waveguide Components using Tollens Reaction Silver Plating

Alexander Simonovic, Egmont Rohwer, and Tinus Stander, *SMIEEE*

***Abstract*—Dielectric printed and plated waveguide components offer cost and weight benefits over metal printed equivalents, with silver plating using Tollens reagents holding significant advantages over electroplating. This work extends on previous demonstrations of this process in plating stereolithography (SLA) printed resin waveguide parts by investigating number of plating rounds, reaction temperature and plastic base. It is found that less than 1.5 dB/m attenuation is achievable in WR42 waveguide using white SLA plastic and silver plating, comparing favourably with the 10 dB/m achieved by printing the same part using Ti64 powder bed fusion. This process improvement is further demonstrated using waveguide power dividers, slow-wave delay sections and rectangular horn antennas.**

***Index Terms*— Additive manufacturing, metal plating, silver plating, stereolithography, Tollens reaction, waveguide components.**

I. Introduction

ADDITIVELY manufactured microwave and mm-wave waveguide components have become more common in recent years [1]. The most evident method for creating metal waveguide parts is through direct metal printing technologies such as selective laser melting (SLM) [2]. This technique has been applied to a variety of microwave components [3]–[6], offering the advantage of easily manufacturable mono-block components in an already conductive material. SLM printing is, however, an expensive process, with components typically suffering from higher surface roughness compared to machined parts [7].

In contrast to direct metal printing, waveguide parts manufactured through dielectric printing and metal plating enable low cost and lightweight systems, especially for satellite applications [8], [9]. Simple dielectric printing technologies such as fused deposition modelling (FDM) and stereolithography (SLA) do not require the costly post-processing that is needed for binder jet printing, with SLA further offering finer resolution and lower surface roughness than FDM printing [10]. This is especially true in antenna systems [11] where loss as low as 1.5 dB/m at K-band has been reported [12] comparing favourably with direct metal printing technologies such as SLM.

The metallization of dielectric waveguide parts requires electroless deposition of a conductive layer, either as the waveguide wall or as a conductive seed layer for electroplating [12], [13]. A variety of electroless metal deposition approaches to dielectric-printed waveguide parts have been proposed in literature. A commercial spray metallisation is used in [14] to create the metal layer on a 3D printed part. This process requires flame treating to improve adhesion before the spray metallisation is applied. It also requires that the metallisation spray can reach internal geometries of the part that is being plated such as in [15] where slots are placed in the W-band waveguide. In [11] and [12], a colloidal metal such as nickel or palladium is used as a catalyst to create the metal layer. The disadvantage of this is that the formation of a metal layer on the part requires that there is a direct contact between the catalyst and metal solution that is being plated, which limits the maximum thickness that can be achieved. In [16] it has been shown that colloidal metal catalysts only work if the colloidal metals can bind and attach to the plastic, which typically requires surface etchants, commonly a chrome acid bath. An example of this is the FDM printed parts in [17] where acrylonitrile butadiene styrene (ABS) printing material is used [18], with a modification in [19] allowing for its application on to SLA printed parts. This process, however, requires harsh etchants [20]. Dry sandblasting has been used to replace chemical etching, which has been applied to materials such as those available to SLA printers, but with the disadvantage that internal waveguide features may not be easily accessible [21]. In

In many cases, the electroless layer is too thin or lossy to serve as waveguide wall, necessitating electroplating after the deposition of a conductive seed layer [18]. Metals such as copper, gold, tin and silver have been demonstrated in this role [21]. A difficulty with electroplating is ensuring coverage in parts where anodes cannot be placed. In [22], non-radiating slots were cut in to the side walls of the waveguide to allow for an improved solution flow within the waveguides. Wire anodes were added to the centres of

This work was funded by National Research Foundation of South Africa (NRF) under grant UID114676 and the University of Pretoria Additive Manufacturing for Electronics Systems grant. *(Corresponding author: A. Simonovic).*

A. Simonovic and T. Stander are with the Department of Electrical, Electronic and Computer Engineering, University of Pretoria, Pretoria, South Africa.

E. Rohwer is with the Department Natural and Agricultural Sciences, University of Pretoria, Pretoria, South Africa.

the waveguides to ensure there is a suitable electric field for electroplating.

In [23], a simplified process to plate printed parts with silver is presented. This process uses the Tollens reaction (traditionally used to test for aldehydes) which results in silver forming on surfaces present in the solution that serve either as electroplating seed layer [24] or electrical waveguide. In comparison to other deposition processes, the Tollens reaction is found to be relatively simple and safe, exhibiting loss of 14 dB/m at W-band. Despite its advantages, very little has been published on the refinement of process parameters in using the Tollens reagent to create dielectric printed waveguides. In [25] the plating process is adapted to include palladium colloid, increasing complexity and the cost of manufacturing but resulting in lower waveguide loss of 10 dB/m at the E-band. The experiments in [25] do not investigate process parameters such as the effect of multiple layer deposition rounds, base resin or the application of the process to more complex waveguide parts.

In this work, we extend on previous applications of Tollens reagents to the production of SLA printed waveguide parts. We investigate, for the first time, the influence of the number of silver deposition rounds, reaction temperature, and base resin material on the electrical properties of the finished parts. which extend on prior efforts in e.g. [21] to create mm-wave waveguides using a Tollens reagent silver layer as a final conductive layer, as opposed to a seed layer for electroplating [22]. We also demonstrate the process on a variety of waveguide components for the first time, including T-junctions, horn antennas, and complex sinusoidal time delay sections.

The paper is organized as follows:
Section II provides details on the printing and silver plating procedure. Section III describes the microwave components that were used to test the silver plating process. Section IV presents the results describing the performance of the silver plating on WR42 straight section waveguide, including an investigation into varying process parameters. Section V presents the results of the silver plating on all the other components presented in Section III. The findings are then concluded in section VI.

II. Fabrication Procedure

Dielectric parts were printed and post-processed using a Fromlabs From 3 printer [26] and the associated wash and cure station. Although parts are sometimes predistorted sometimes to compensate for printing error [27], predistortion was not used here. Parts followed the recommended post-processing steps, including a 10-minute rinse in isopropyl alcohol (IPA) in a Form Wash and curing for 60 minutes and 60°C in the Form Cure solution. For this experiment, the white and clear resins from Form Labs were used [28]. The white resin was investigated because it offers an accuracy of 50 µm with minimal post-processing and is recommended by the manufacturer for parts that undergo surface finishing. The use of clear resin was also investigated, as it is capable of an accuracy of 25 µm, which may improve surface finishes.

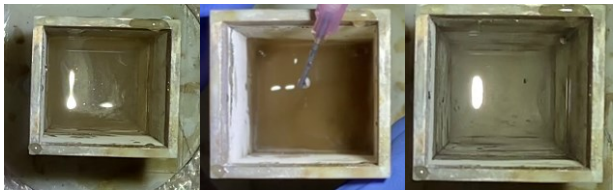

Fig. 1. Colour change of the plating liquid when adding NH_4OH. The left image shows silver nitrate before adding NH_4OH. The center image is while the NH_4OH is being added. The right image show the solution after enough NH_4OH has be added.

After printing and curing, the parts are first cleaned of any oils, whilst handling the parts with gloves to prevent oil transfer from skin contact. This is done through ultrasonic agitation for 15 minutes in acetone, then in methanol, and finally in isopropyl alcohol (IPA), with parts dried at 50°C between each cleaning stage.

After curing, parts were subjected to the silver-plating process described in Fig. 2. A solution of 25 ml distilled water and 0.5 g $AgNO_3$ was first poured into a plating container, after which NH_4OH was added drop-wise to the $AgNO_3$ solution, with the solution turning brown after a few drops. NH_4OH was added until the solution became clear again (Fig. 1). Next, 0.35 g of NaOH dissolved into 25 mL of distilled water was added into the container, which turned the mixture brown. Again, NH_4OH was added dropwise until the solution became clear once again. The solution was gently agitated during each NH_4OH addition to ensure that the solutions were mixed well.

After preparing the solution, the part was submersed in the solution, oriented to avoid trapped air and gently agitated to loosen any air bubbles on the surface of the part. After all the bubbles were removed from the surface of the part, 0.4 g of dextrose dissolved in 10 ml of distilled water was added while swirling the solution to ensure that the dextrose was mixed throughout the solution. The colour changed from clear to grey over a span of 5 minutes, seen in Fig. 3. The part was left in the solution for 10 minutes until the solution started to become clear, after which the part was rinsed and kept in water until the next round of silver was deposited.

It was found that the deposition time was relatively brief, during which all of the silver had reacted, and the deposition ceased spontaneously. To increase the silver layer thickness, and improve coverage, parts had to undergo multiple rounds of the Tollens reaction. The number of required plating rounds was investigated as a process

variable. Parts with complex internal geometry were found to reduce flow of the plating solution, requiring additional rounds of plating.

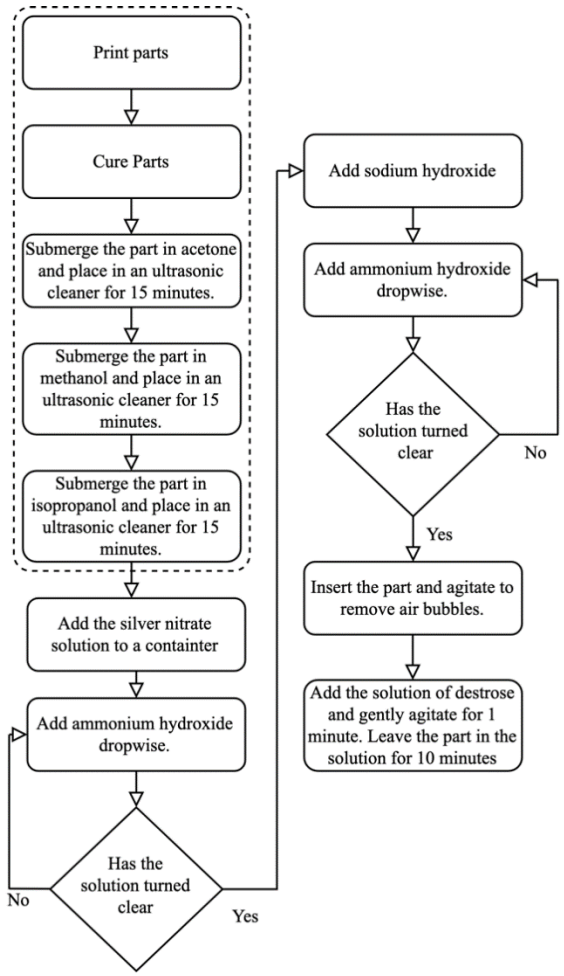

Fig. 2. Process flow diagram for Tollens silver plating.

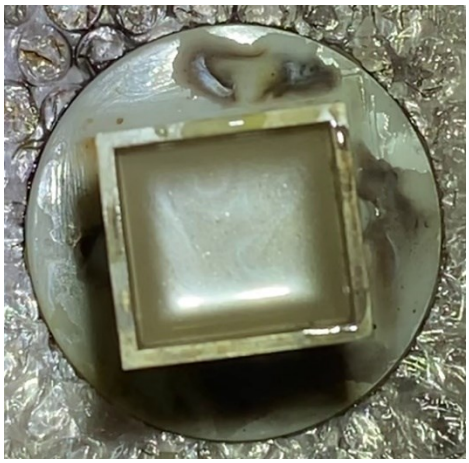

Fig. 3. Plating solution after five minutes of reacting. The parts cannot be seen because of the silver in the solution.

It was further established that hydrophilic resins allow for improved contact between the Tollens solution and the printed parts. Hydrophilicity depends on resin synthesis, which means that some resins (the exact composition of which is usually proprietary and unknown) may feature better adhesion to silver from the Tollens reaction than others. A hydrophilic resin would further increase the amount of silver that forms on the parts for every round of the tollens reaction. This informed the investigation of different resins in creating the parts.

III. Devices Under Test

To demonstrate the efficacy of the process with a variety of geometries, a range of WR42 waveguide parts were manufactured, for operation in the 18 – 27 GHz K-band as constituent parts of a series-fed phased array antenna. This band is commonly used for satellite communications [8], [9] and is often cited as an application of additively manufactured (AM) waveguide components.

Initial designs made use of split block in an attempt to avoid poor coverage on internal surfaces, as done in e.g. [13], [24]. However, successive attempts showed that it was not necessary to use split block assembly for the silver plating process that is used here, simplifying the manufacturing process.

A. Straight Waveguide Sections

The primary test structure was a length of standard WR42 waveguide (10.668 × 4.318 mm internal dimensions) of 100 mm in length and 1 mm wall thickness, with standard FBP220 square flange dimensions. This was selected to allow for fair comparison to other AM processes in literature [29], [30].

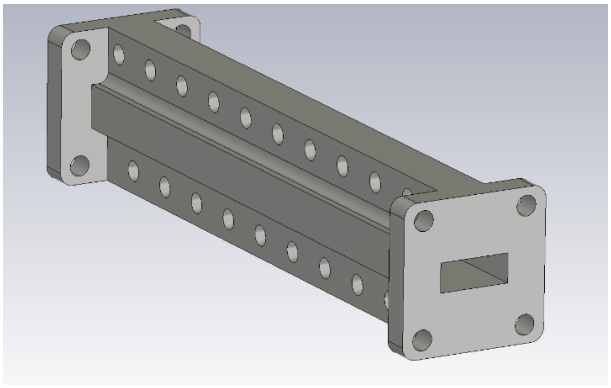

Fig. 4. Straight waveguide section design that is used in this work.

B. Time Delay Sections

To investigate silver adhesion to complex internal waveguide geometries, two sinusoid ridge time delay sections [31] were produced, with cosine tapers from the WR42 port to the internal ridge pattern. The sections were designed for 0.628 ns and 0.429 ns delay over 100 mm length, respectively, with typical minimum ridge clearance of 1.44 mm.

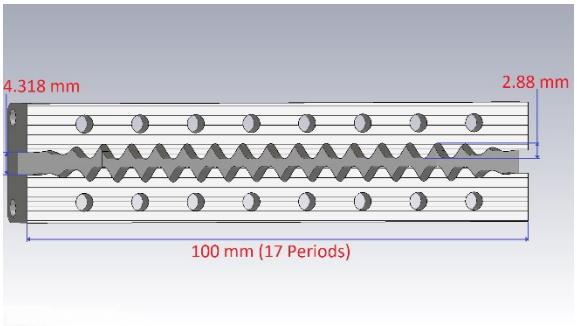

Fig. 5. Sectioned view of waveguide time delay section.

C. Power Dividers

Three WR42 reactive T-junction power dividers [32] were manufactured, with power split ratios of 1:3, 1:2 and 1:1 achieved by varying the internal septum and iris dimensions. The minimum internal aperture dimensions were 5.97 mm × 4.318 mm for the 3:1 divider. A section top view of the power divider is shown in Fig. 6. The divider is symmetrical around the section view.

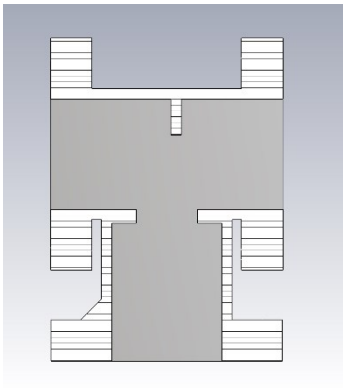

Fig. 6. Waveguide Power Divider

D. Rectangular Waveguide Horn Antenna.

Finally, a 13.3 dBi gain WR42 waveguide horn was manufactured (Fig. 6), to investigate the plating process's influence on radiation properties. The horn has an aperture size of 19.47 mm × 17.24 mm, with a length of 37.25 mm and wall thickness of 1 mm.

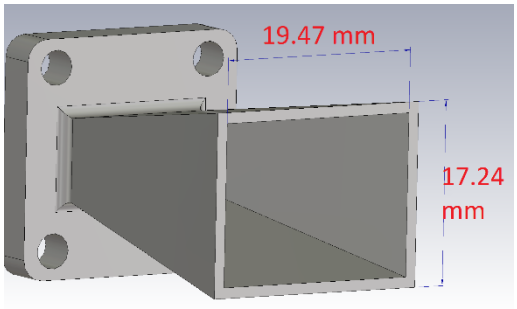

Fig. 7. Horn Antenna

IV. Parametric Variations in Manufacturing Process

Before creating the final plated DUTs, a parametric study was conducted on different plating process choices. The S-parameters of the 100 mm length WR42 waveguide section is used to discriminate between plating choices, with S_{21} commonly used as a loss metric in these experiments in literature [13], [23], [25]. The S-parameters were measured on an Anritsu MS4647A VNA from 18 GHz to 27 GHz (Fig. 8), using Short-offset-Short-Load-Through (SSLT) calibration at the flanges with six sliding load measurements.

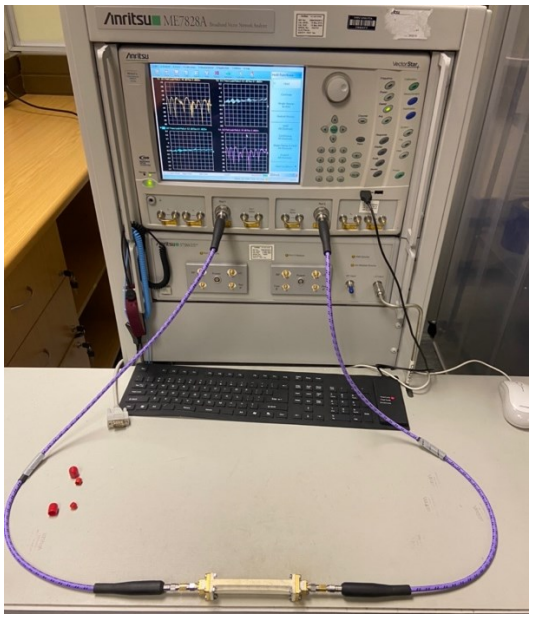

Fig. 8. Straight section being measured on the VNA.

A. Base resin comparison

The results in Fig. 9 show a comparison between waveguides printed in the white and clear resin offered by Formlabs with 4 rounds of plating. As the parts are air-filled and completely metallized, the dielectric properties of the material are not a performance consideration. Instead, the different base materials are compared for adhesion and uniformity of the silver plating, which alter the outer conductivity of the part and manifest as transmission and reflection loss. The higher reflection coefficient of the clear resin waveguide, when compared to the white resin, is attributed to a poorer flange contact interface. However, reflection alone does not explain the low transmission, which may be the result of extreme absorption or radiation loss due to a poor silver plating finish in the corners of the clear waveguide (Fig. 10).

This result was found consistently in experimentation, and as such, all subsequent experiments were conducted with the Formlabs white resin.

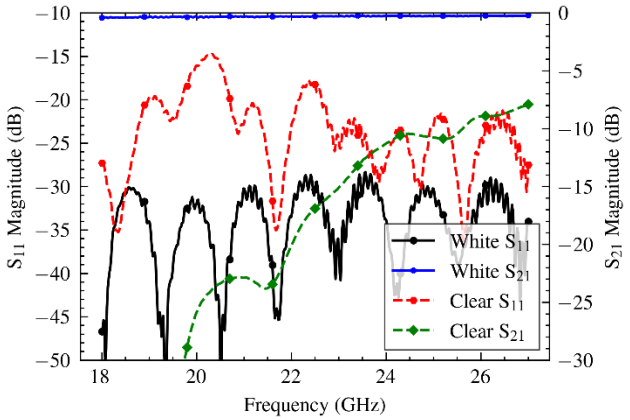

Fig. 9. S-parameter results of white and clear resin straight sections.

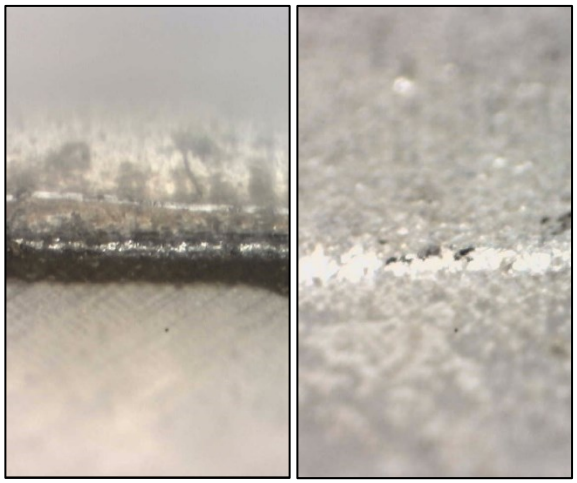

Fig. 10. Oxidation in the corners of a clear resin waveguide (left) vs the corners found in white resin waveguide (right).

B. Number of plating rounds

The coverage and thickness of the silver layer is affected by the number of silver rounds the part undergoes. Waveguide transmission response was considered the most direct measure of the effective RF conductivity of the layer, as dc sheet resistance fails to account for the skin effect. As a start, to examine plating thickness explicitly, glass slides were plated with a varying number of rounds ranging from one to five. Glass was used because for low surface roughness, making the thickness of the silver layer more distinct. Plastic slides were attempted but the surface roughness of the printed plastic masked the thickness of the silver layer. The results in Table I would indicate a significant increase in silver layer thickness up to 3 rounds of plating, with modest increases up to 5 rounds. A

minimum thickness of 2 µm was maintained for both 4 and 5 rounds of plating.

Table I
Silver Thickness for Differing Number of Silver Plating Rounds.

Number of Rounds	Average thickness (µm)	Minimum thickness (µm)
5	7.54	2
4	6.76	2
3	6.93	1.22
2	2.87	1
1	0.6	NA

Considering that the skin depth of silver is 0.423 µm at 22.5 GHz, 3 layers of plating would equate to 16.4 skin depths, while 5 layers would lead to 17.8 skin depths or 99.99% of the total surface current distribution. It was further found that one round of plating did not create a consistent layer of silver, with holes clearly evident in the coating (Fig. 11).

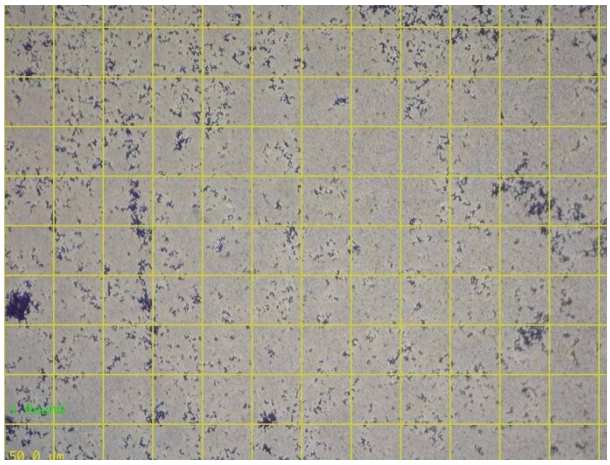

Fig. 11. Microscope image of the silver surface on the glass slides after one round. Dark areas indicate holes in the silver plating. Grid spacing is 50 µm.

In contrast, the surface with four rounds of plating is shown in Fig. 12, indicating a textured, but consistent plating surface.

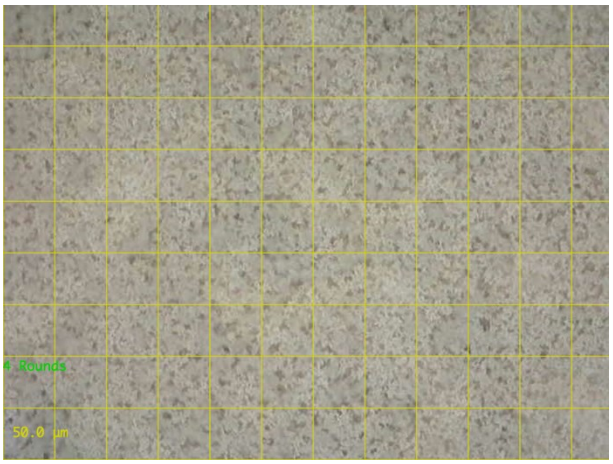

Fig. 12. Microscope image showing the silver surface with four rounds of plating. The surface is textured but has no holes. Grid spacing is 50 µm.

Subsequently, the straight waveguide DUT underwent 6 rounds of silver plating with measurements taken after each plating round. In Fig. 13, the input reflection S_{11} for 1 – 4 rounds is shown, indicating significantly reduced contact resistance and lower reflection at the flange after four rounds of plating. From the transmission responses for 1 – 4 rounds shown in Fig. 14, it is evident that sufficient coverage for an effective internal electric wall is only attained after four plating rounds, which is subsequently applied throughout the study.

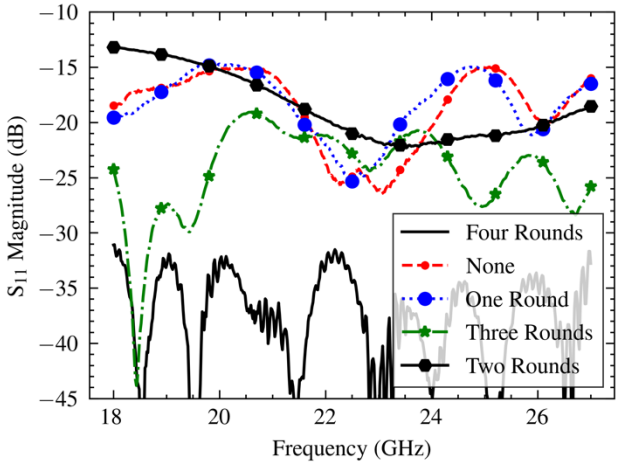

Fig. 13. Measured S_{11} of white resin waveguides after multiple rounds of silver plating.

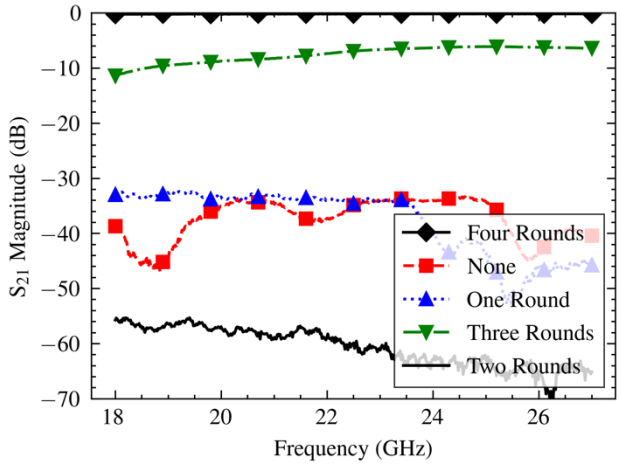

Fig. 14. Measured S_{21} of white resin waveguides after multiple rounds of silver plating.

The transmission responses for 4 – 6 rounds of plating in Fig. 15 would indicate that further plating after four rounds does not hold much benefit. While the improvement in transmission magnitude from three rounds to four rounds is 70 – 100 dB/m, the improvement from four rounds to five is only 0.7 dB/m and only 0.2 dB/m when comparing five and six rounds. A minimum of 1 dB/m was achieved over the band with six plating rounds, with less than 2.4 dB/m over the band achieved with four rounds.

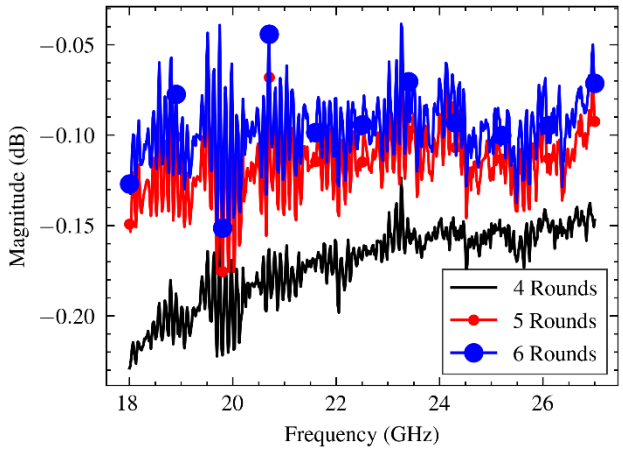

Fig. 15. Transmission loss with more than four rounds of silver plating.

C. Minimising oxidation

In [33] the performance degradation of a silver plated waveguide is investigated. It was found that oxidation had a minor, but measurable effect on loss. In this experiment, it was found that silver plated parts experience some oxidation, visible as black or darker discolouration. The reaction rate was slowed [34] through lowering the reaction temperature to 10˚C by refrigerating the solution before plating, though a systematic study of the effect of reaction temperature was not conducted. Air exposure between plating rounds was also reduced by placing the parts in distilled water during the preparation [35] and immediately after each plating round. By not using the oven to dry the parts, oxidation (due to increased temperature) is reduced.

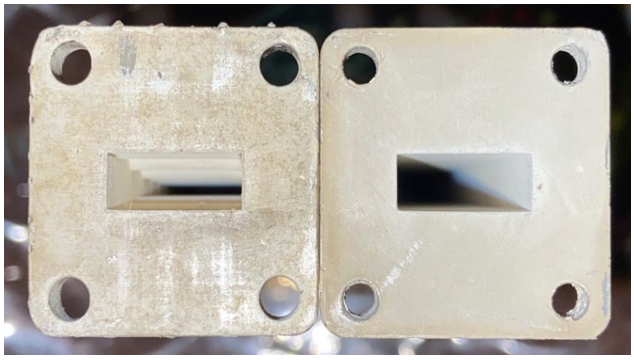

Fig. 16. Comparison of two waveguide manufactured at different temperatures. The waveguide that is dried in an oven (left) shows a less uniform surface finish than the waveguide that is kept in distilled water (right).

In Fig. 16, two waveguide flanges are shown. The waveguide on the left was dried in the oven and left in open air between plating rounds, while the waveguide on the right was kept in cooled distilled water as well as plated at a lower temperature. Making the parts this way improved the performance of the part slightly, producing loss of only 2.1 dB/m instead of 2.4 dB/m.

V. Straight Section Characterisation Results

In Fig. 17 and Fig. 18, the silver-plated SLA waveguide with four rounds of plating is compared to a commercial off-the-shelf section of waveguide and a metal-printed waveguide of the same length. The commercial waveguide is manufactured in copper with silver plating, while the SLM-printed waveguide was manufactured using an EOS EOSINT M290 and EOS Titanium Ti64 Grade 23 powder, with the flanges skimmed to reduce the surface roughness but otherwise left untreated.

While the SLA waveguide features marginally higher input reflection than the others (attributed to slight corner rounding or flange offset [36]), as shown in Fig. 17, the insertion loss of the SLA waveguide compares well to that of the commercial waveguide (which featured below 1 dB/m loss). The higher loss in the SLM part may be attributed to the surface roughness [37] and may be improved on further with polishing between plating rounds [38]. However, considering the comparison to other additively manufactured waveguides in TABLE II, it is evident that this process already produces waveguide with competitive performance at K-band.

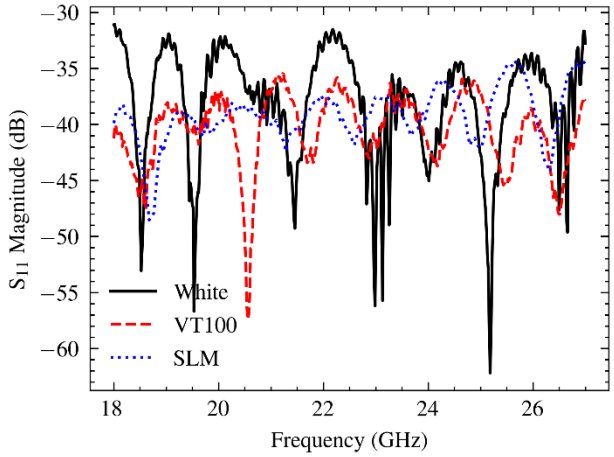

Fig. 17. Comparison of S_{11} between a white SLA waveguide, an off-the-shelf waveguide (VT100) and a metal printed waveguide.

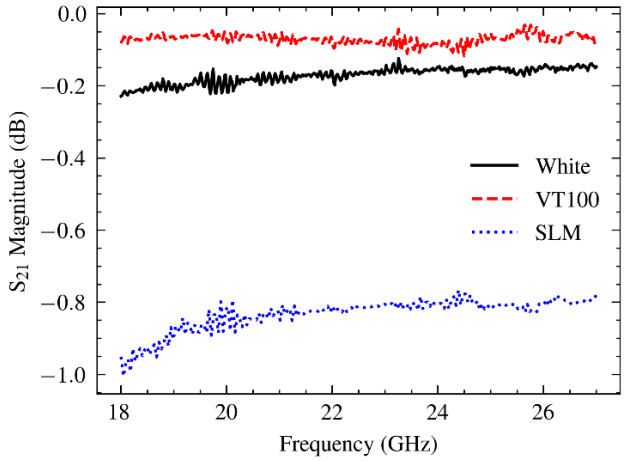

Fig. 18. Comparison of S_{21} between a white SLA waveguide, an off the shelf waveguide (VT100) and a metal printed waveguide.

TABLE II
Comparison of Additively Manufactured Waveguides.

Source	Loss dB/m @ Frequency	Plating Type
[39]	4.3 dB/m @ Ka-band	Binder Jetting with metal infiltration
[23]	14 dB/m @ 75-110 GHz	SLA with Tollens silver plating (original)
[29]	11 dB/m @ K-band	Silver ink dispensing on FDM
[10]	1.29 dB/m @ Ku-band	FDM with liquid metal filling
[3]	0.58 dB/m @ X-band	FDM ABS with copper electroplating
[5]	3.75 dB/m @ X-band	SLS printing
This Work SLA	2.1 dB/m @ K-band	SLA with 4 rounds of Tollens silver plating
This work SLM	10 dB/m K-band	SLM titanium printing

Multiple straight sections were manufactured to determine the repeatability of the process. Mid-band variation of ~2 dB/m is evident, with a worst-case insertion loss of below 4.5 dB/m mid-band (Fig. 19).

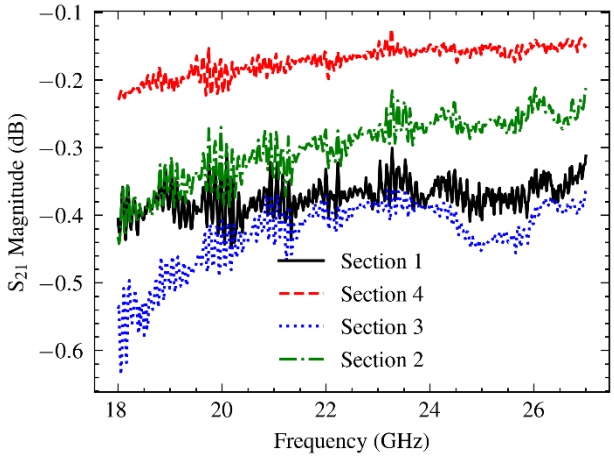

Fig. 19. Transmission response of multiple identical straight section waveguides.

The cost of the non-reusable material used to plate the straight waveguide sections (16.4 cm^3) totalled $17.00 when four rounds of silver are used, which is substantially cheaper than direct metal printing or conventional machining or extrusion.

VI. Experimental Results of other DUTs

Using the best-practice plating process choices established by experimentation in the previous section, the other DUTs were subsequently printed and plated. The time delay sections, and power dividers were measured in the same manner as the straight waveguide sections, while the horn antennas were measured in a compact range, with full azimuth and elevation patterns taken every at 250 MHz intervals between 18 and 27 GHz. All simulations were performed in CST Microwave Studio 2022, using the time domain solver.

A. Time Delay Sections

The transmission of the three delay sections are shown in Fig. 20, clearly (and expectedly) indicating more loss in the longer delay section. To achieve the results shown here, the branch with the greatest time delay underwent eight silver plating rounds. This example illustrates the need for more plating rounds in complex geometries with narrow internal clearance dimensions. Branches 2 and 3 were design to have very similar delay characteristics but branch 2 was not subjected to extra rounds of plating like branch 3. This is evident in the figure, where branch 3 features much lower loss than branch 2.

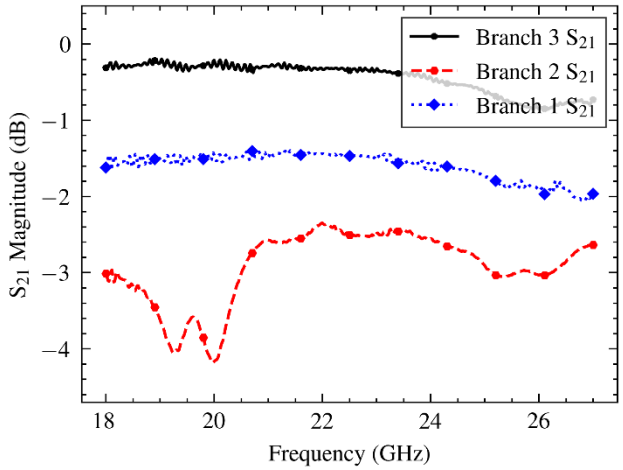

Fig. 20. S_{21} Measurement of the time delay sections.

The group delay results are shown in Fig. 21, and compare well to simulated values. The fewer plating rounds of branch 2 did not significantly affect the achieved group delay when considering how closely branch 3 matches its simulated response.

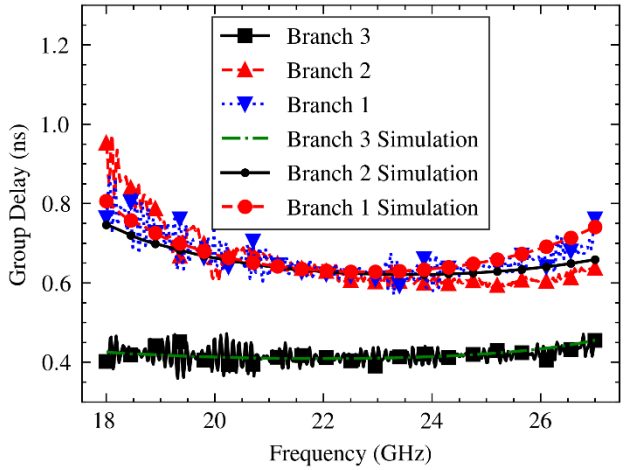

Fig. 21. Group Delay of the time delay sections.

B. Power Dividers

The simulated and measured results of the 3:1, 2:1 and 1:1 power dividers are shown in Fig. 22, Fig. 23 and Fig. 24, respectively, with less than 0.2 dB difference in the transmission responses (S_{21} and S_{31}) in all cases. The printed parts feature marginally higher input reflection at the lower band edge compared to simulation.

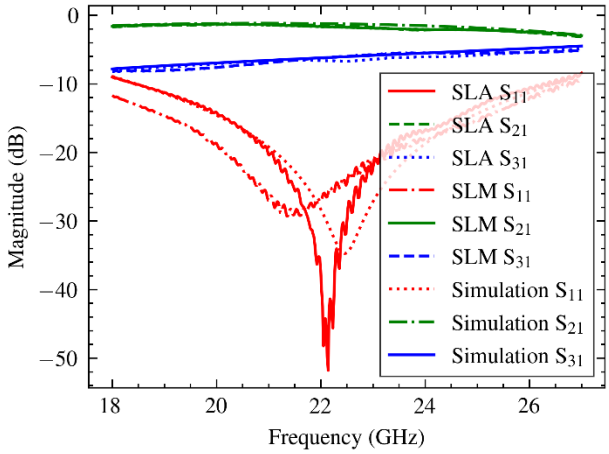

Fig. 22. First divider with a power division of 3:1.

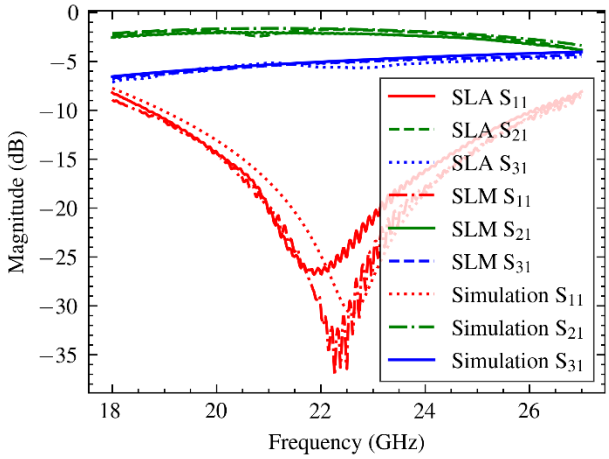

Fig. 23. Second power divider with a division of 2:1.

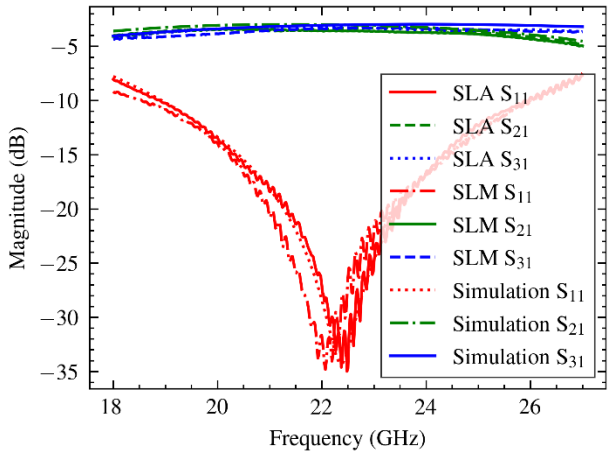

Fig. 24. Third power divider with a division of 1:1.

C. Horns

In the final DUT experiment, the gain of the SLA printed horn is compared to an SLM printed equivalent. The comparison of co-polarisation gains in Fig. 25 indicates excellent agreement in radiated properties, with the SLA part featuring 12.93 dBi boresight gain compared to 12.89 dBi for the SLM printed horn and 13.25 dBi in simulation.

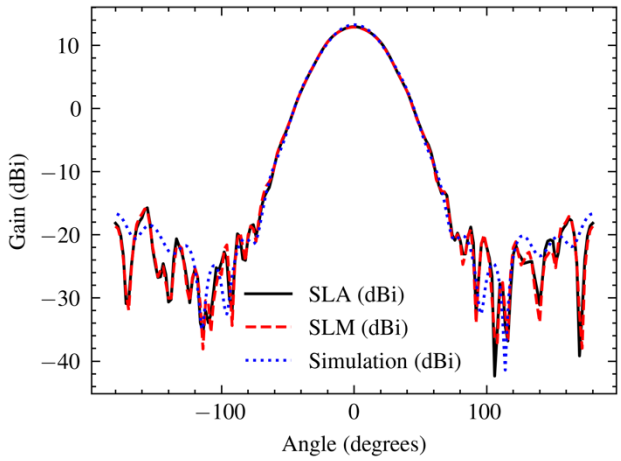

Fig. 25. Comparison of SLA, SLM and simulated horns during an azimuth sweep measuring co-polarisation.

The cross-polar gain is shown in Fig. 26. The non-negligible cross-polar gain (evident in both antennas at around -10 dBi) may be attributed to minor printing deformation which is visible when looking into the horn flange.

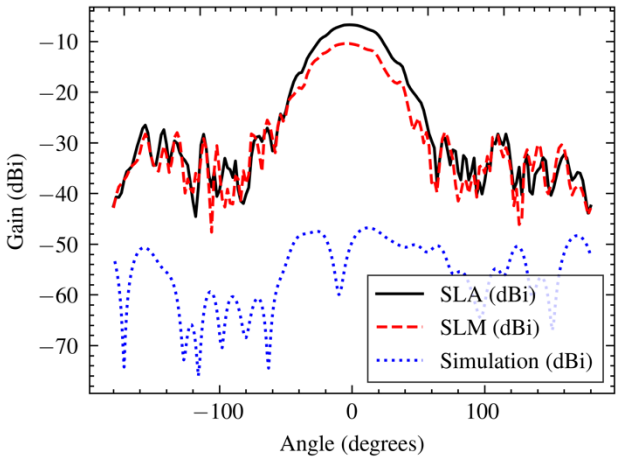

Fig. 26. Cross polar radiation measurement.

The boresight gains for the SLM and SLA printed antennas are shown in Fig. 27, and match closely. The SLA horn has a marginally larger gain than the SLM horn antenna, most likely a result of the surface roughness of the SLM printed parts.

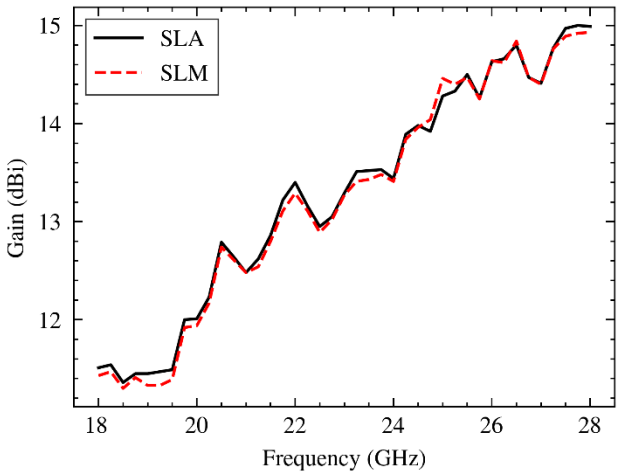

Fig. 27. Boresight gain versus frequency for the SLA and SLM printed horn antenna.

VII. Conclusion

We have presented, for the first time, a detailed process guideline and process parametric study on the production of microwave waveguides by SLA dielectric printing and silver deposition by Tollens reaction. It is found that, using a commercial resin with four plating rounds, loss of 2.4 dB/m can be achieved at K-band, with 1.5 dB/m achievable with six plating rounds. This compares extremely well with the 4.3 dB/m at K-band achievable with binder jetting, while being much cheaper at $17.71 per part. It also shows that the process is suitable to plating waveguide parts with

complex internal geometries and produces horn antennas with negligible reduction in radiation efficiency compared to simulation.

Future work may investigate the effect of pumping the plating solution through the waveguide during the reaction, as well as investigate the reliability of the parts (in particular, the peel strength of the silver layer) under temperature variation, shock and vibration.

ACKNOWLEDGMENT

The authors wish to thank the Centre for Rapid Prototyping and Manufacturing (CRPM) at the Central University of Technology (CUT) for manufacturing the SLM prototypes used as comparison examples in this work.

REFERENCES

[1] C. Tomassoni, O. A. Peverini, G. Venanzoni, G. Addamo, F. Paonessa, and G. Virone, "3D Printing of Microwave and Millimeter-Wave Filters: Additive Manufacturing Technologies Applied in the Development of High-Performance Filters with Novel Topologies," *IEEE Microw Mag*, vol. 21, no. 6, pp. 24–45, Jun. 2020,

[2] B. Zhang and H. Zirath, "Metallic 3-D Printed Rectangular Waveguides for Millimeter-Wave Applications," *IEEE Trans Compon Packaging Manuf Technol*, vol. 6, no. 5, pp. 796–804, May 2016,

[3] M. D'Auria *et al.*, "3-D Printed Metal-Pipe Rectangular Waveguides," *IEEE Trans Compon Packaging Manuf Technol*, vol. 5, no. 9, pp. 1339–1349, Sep. 2015,

[4] P. Vaitukaitis, K. Nai, J. Rao, and J. Hong, "3D Metal Printed Deformed Elliptical Cavity Bandpass Filter with an Additional Plate," in *2021 IEEE CPMT Symposium Japan (ICSJ)*, Nov. 2021, pp. 118–119.

[5] G.-L. Huang and T. Yuan, "Application of 3-D metal printing to microwave components and antennas," in *2017 Sixth Asia-Pacific Conference on Antennas and Propagation (APCAP)*, Oct. 2017, pp. 1–3.

[6] J. J. P. Venter, A.-L. Franc, T. Stander, and P. Ferrari, "Transmission lines characteristic impedance versus Q-factor in CMOS technology," *Int J Microw Wirel Technol*, pp. 1–6, 2021,

[7] C. Tomassoni, O. A. Peverini, G. Venanzoni, G. Addamo, F. Paonessa, and G. Virone, "3D Printing of Microwave and Millimeter-Wave Filters: Additive Manufacturing Technologies Applied in the Development of High-Performance Filters with Novel Topologies," *IEEE Microw Mag*, vol. 21, no. 6, pp. 24–45, Jun. 2020,

[8] L. Polo-López *et al.*, "Waveguide Manufacturing Technologies for Next-Generation Millimeter-Wave Antennas," *Micromachines (Basel)*, vol. 12, no. 12, p. 1565, Dec. 2021,

[9] O. A. Peverini *et al.*, "Manufacturing of waveguide components for SatCom through selective laser melting," in *2017 11th European Conference on Antennas and Propagation (EUCAP)*, Mar. 2017, pp. 563–566.

[10] K. Y. Chan, R. Ramer, and R. Sorrentino, "Low-Cost Ku-Band Waveguide Devices Using 3-D Printing and Liquid Metal Filling," *IEEE Trans Microw Theory Tech*, vol. 66, no. 9, pp. 3993–4001, Sep. 2018,

[11] G. P. Le Sage, "3D Printed Waveguide Slot Array Antennas," *IEEE Access*, vol. 4, pp. 1258–1265, 2016,

[12] R. Zhu and D. Marks, "Rapid prototyping lightweight millimeter wave antenna and waveguide with copper plating," in *2015 40th International Conference on Infrared, Millimeter, and Terahertz waves (IRMMW-THz)*, Aug. 2015, pp. 1–2.

[13] R. Zhu, G. Lipworth, T. Zvolensky, D. R. Smith, and D. L. Marks, "Versatile Manufacturing of Split-Block Microwave Devices Using Rapid Prototyping and Electroplating," *IEEE Antennas Wirel Propag Lett*, vol. 16, pp. 157–160, 2017,

[14] S. Alkaraki, Y. Gao, S. Stremsdoerfer, E. Gayets, and C. G. Parini, "3D Printed Corrugated Plate Antennas With High Aperture Efficiency and High Gain at X-Band and Ka-Band," *IEEE Access*, vol. 8, pp. 30643–30654, 2020,

[15] J. Tak, A. Kantemur, Y. Sharma, and H. Xin, "A 3-D-Printed <italic>W</italic>-Band Slotted Waveguide Array Antenna Optimized Using Machine Learning," *IEEE Antennas Wirel Propag Lett*, vol. 17, no. 11, pp. 2008–2012, Nov. 2018,

[16] C. Bachiller *et al.*, "Additive manufacturing and metallization of high-frequency communication devices," *Progress in Additive Manufacturing*, Jan. 2023,

[17] K. Ruskova, T. Pavlov, B. Tzaneva, and P. Petkov, "Electroless Copper Deposition for Antenna Applications," in *2018 IX National Conference with International Participation (ELECTRONICA)*, May 2018, pp. 1–4.

[18] S. Olivera, H. B. Muralidhara, K. Venkatesh, K. Gopalakrishna, and C. S. Vivek, "Plating on acrylonitrile–butadiene–styrene (ABS) plastic: a review," *J Mater Sci*, vol. 51, no. 8, pp. 3657–3674, Apr. 2016,

[19] E. G. Geterud, P. Bergmark, and J. Yang, "Lightweight waveguide and antenna components using plating on plastics," in *2013 7th European Conference on Antennas and Propagation (EuCAP)*, 2013, pp. 1812–1815.

[20] X. Han, G. Wang, J. He, J. Guan, and Y. He, "Influence of temperature on the surface property of

ABS resin in KMnO 4 etching solution," *Surface and Interface Analysis*, vol. 51, no. 2, pp. 177–183, Feb. 2019,

[21] F. Le Borgne, G. Cochet, J. Haumant, D. Diedhiou, K. Donnart, and A. Manchec, "An Integrated Monobloc 3D Printed Front-end in Ku-band," in *2019 49th European Microwave Conference (EuMC)*, Oct. 2019, pp. 786–789.

[22] K. Zhao, J. A. Ramsey, and N. Ghalichechian, "Fully 3-D-Printed Frequency-Scanning Slotted Waveguide Array With Wideband Power-Divider," *IEEE Antennas Wirel Propag Lett*, vol. 18, no. 12, pp. 2756–2760, Dec. 2019,

[23] J. Shen, M. Aiken, C. Ladd, M. D. Dickey, and D. S. Ricketts, "A simple electroless plating solution for 3D printed microwave components," in *2016 Asia-Pacific Microwave Conference (APMC)*, Dec. 2016, pp. 1–4.

[24] A. Simonovic, E. Rohwer, and T. Stander, "SLA Printed K-Band Waveguide Components using Tollens Reaction Silver Plating," in *The International Conference on Electromagnetics in Advanced Applications*, Jun. 2022, pp. 1–4.

[25] K. Lomakin *et al.*, "SLA-Printed 3-D Waveguide Paths for E-Band Using Electroless Silver Plating," *IEEE Trans Compon Packaging Manuf Technol*, vol. 9, no. 12, pp. 2476–2481, Dec. 2019,

[26] F. Labs, "High Performance 3D Printers," 2022. https://formlabs.com/ (accessed Mar. 15, 2022).

[27] S. Afazov, E. Semerdzhieva, D. Scrimieri, A. Serjouei, B. Kairoshev, and F. Derguti, "An improved distortion compensation approach for additive manufacturing using optically scanned data," *Virtual Phys Prototyp*, vol. 16, no. 1, pp. 1–13, Jan. 2021,

[28] F. Labs, "Materials for High Resolution Models and Rapid Prototyping," *Onlline*, 2022. https://formlabs.com/materials/standard/ (accessed Mar. 15, 2022).

[29] S. Khan, N. Vahabisani, and M. Daneshmand, "A Fully 3-D Printed Waveguide and Its Application as Microfluidically Controlled Waveguide Switch," *IEEE Trans Compon Packaging Manuf Technol*, vol. 7, no. 1, pp. 70–80, Jan. 2017,

[30] O. A. Peverini *et al.*, "Additive manufacturing of Ku/K-band waveguide filters: a comparative analysis among selective-laser melting and stereo-lithography," *IET Microwaves, Antennas & Propagation*, vol. 11, no. 14, pp. 1936–1942, Nov. 2017,

[31] X. Xu *et al.*, "Sine Waveguide for 0.22-THz Traveling-Wave Tube," *IEEE Electron Device Letters*, vol. 32, no. 8, pp. 1152–1154, Aug. 2011,

[32] S. H. Lee, J. S. Kim, Y. J. Yoon, and W. S. Lee, "Six-way power divider for series feed using H-plane T-junctions," *Microw Opt Technol Lett*, vol. 58, no. 7, pp. 1622–1626, Jul. 2016,

[33] V. P. Turyanskii, É. A. Kashtanova, and Yu. I. Demidov, "Tests of waveguide platings," *Measurement Techniques*, vol. 29, no. 1, pp. 46–48, 1986,

[34] A. Antonello *et al.*, "Optimized Electroless Silver Coating for Optical and Plasmonic Applications," *Plasmonics*, vol. 7, no. 4, pp. 633–639, Dec. 2012,

[35] M. L. Zheludkevich, A. G. Gusakov, A. G. Voropaev, A. A. Vecher, E. N. Kozyrski, and S. A. Raspopov, "Oxidation of Silver by Atomic Oxygen," *Oxidation of Metals*, vol. 61, no. 1, pp. 39–48, 2004,

[36] H. Li, "Waveguide flange design and characterization of misalignment at submillimeter wavelengths," Doctoral Dissertation, Feb, 2013.

[37] N. Clark, S. Hefford, and A. Porch, "Effect of build orientation and surface finish on surface resistance in microwave components produced by Selective Laser Melting," in *2017 47th European Microwave Conference (EuMC)*, Oct. 2017, pp. 508–511.

[38] F. Zhang *et al.*, "3-D Printed Slotted Spherical Resonator Bandpass Filters With Spurious Suppression," *IEEE Access*, vol. 7, pp. 128026–128034, 2019,

[39] E. A. Rojas-Nastrucci, J. T. Nussbaum, N. B. Crane, and T. M. Weller, "Ka-Band Characterization of Binder Jetting for 3-D Printing of Metallic Rectangular Waveguide Circuits and Antennas," *IEEE Trans Microw Theory Tech*, vol. 65, no. 9, pp. 3099–3108, Sep. 2017,

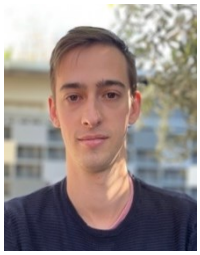

Alexander Simonovic received the B. Eng degree in Electronic Engineering in 2020, and B. Eng (Hons) in 2021, at the University of Pretoria (UP), South Africa. He is currently a Master's degree student at the Department of EEC Engineering at UP, with research interests in antenna array design and additive manufacturing. He also served as an assistant lecturer at the University of Pretoria.

Egmont Rohwer received his MSc, University of Stellenbosch 1978 and PhD in Chemistry, Rand Afrikaans University (now University of Johannesburg) 1982. Professor of Chemistry since 1985 and former Head of the Department of Chemistry at

the University of Pretoria. He specialises in Mass Spectrometry and Chromatography to establish the chemical composition of complex mixtures. This is done to address research problems in fields ranging from engineering, biology, geology and archaeology to forensic, environmental, medical and food sciences. He has recently also initiated a long-term project aiming to convert renewable energy and CO2 to liquid fuels via electrocatalysis. He finds the greatest challenge in designing new instrumentation and developing customized analytical methods to i.a. research pheromone communication in insects, environmental pollution, wine aroma, lubricants in synthetic diesel fuel and diagnosis of disease.

Tinus Stander (Senior Member, IEEE) received the B.Eng. and Ph.D. degrees in electronic engineering from the University of Stellenbosch, Stellenbosch, South Africa, in 2005 and 2009, respectively. From 2010 to 2012, he was an RF and Microwave Engineer with Denel Dynamics (a division of Denel SOC Ltd.), Irene, South Africa, before joining the Carl and Emily Fuchs Institute for Microelectronics, Department of Electrical, Electronic and Computer Engineering, University of Pretoria, Pretoria, South Africa, in 2013. He currently serves as a Professor and the Institute's Principal Investigator for microwave and mm-wave electronics and microelectronics, with personal research interests in the application of electromagnetics in MMIC design, built-in self-testing, and low-cost mm-wave system realization. He is also registered as a Professional Engineer with the Engineering Council of South Africa and consults as Scientific Advisor at Multifractal Semiconductors (Pty.) Ltd., Pretoria.